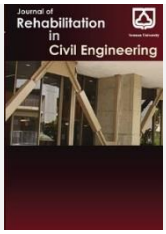

Journal of Rehabilitation in Civil Engineering

Journal homepage: https://civiljournal.semnan.ac.ir/

Enhancing Pervious Concrete for Sustainable Urban Stormwater Management: A Novel Mix Design Approach with Local Pozzolans and Polypropylene Fibers

Mahmood Taghdisi Elli [1]; Kazem Esmaili [2,*]; Saeed Reza Khodashenas [3]; Seyed Ali Ziaee [4]; Saeed Fatemi [5]

1. Ph.D. candidate, water science and engineering, Ferdowsi University of Mashhad, Mashhad, Iran
2. Associate Professor, water science and engineering, Ferdowsi University of Mashhad, Mashhad, Iran
3. Professor, water science and engineering, Ferdowsi University of Mashhad, Mashhad, Iran
4. Assistant Professor, Department of Civil Engineering, Faculty of Engineering, Ferdowsi University of Mashhad, Mashhad, Iran
5. Ph.D., Department of Civil Engineering, Faculty of Engineering, Ferdowsi University of Mashhad, Mashhad, Iran
* Corresponding author: *esmaili@um.ac.ir*

ARTICLE INFO

Article history:
Received: 04 February 2025
Revised: 09 August 2025
Accepted: 17 August 2025

Keywords:
Pervious concrete;
Local pozzolanic materials;
Sustainable urban drainage systems (SUDS);
Stormwater management;
Mechanical performance.

ABSTRACT

Urbanization significantly reduces the natural permeability of land, which exacerbates issues related to surface runoff and drainage. Pervious concrete serves as a sustainable pavement solution that enhances water infiltration and helps mitigate urban flooding. This study aimed to develop and evaluate innovative mix designs that incorporate locally sourced ceramic and carbide-based pozzolans, along with polypropylene fibers. The optimal mix was identified as consisting of 5% ceramic pozzolan, 5% carbide pozzolan, and polypropylene fibers. This blend demonstrated exceptional properties, achieving a permeability rate of 140,947 mm/h, a compressive strength of 14.5 MPa, a flexural strength of 2.4 MPa, a porosity of 34.8%, and a density of 1,799 kg/m³. When compared to baseline mixes, the pozzolanic blends not only improved mechanical performance but also maintained or enhanced permeability. These results highlight the proposed mix's substantial potential for cost-effective and high-performance applications in sustainable urban drainage systems, ultimately contributing to improved stormwater management in urban settings.

E-ISSN: 2345-4423

How to cite this article:
taghdisielli, M., Esmaili, K., Khodashenas, S. R., Ziaee, S. A. and Fatemi, S. (2026). Enhancing Pervious Concrete for Sustainable Urban Stormwater Management: A Novel Mix Design Approach with Local Pozzolans and Polypropylene. Journal of Rehabilitation in Civil Engineering, 14(2), 2265. https://doi.org/10.22075/jrce.2025.2265

1. Introduction

The United Nations' World Urbanization Prospects shows that over half of the world's population has lived in cities since 2007, a number expected to reach 60% by 2030 and 70% by 2050, with about 95% of this growth occurring in developing countries [1]. This rapid urbanization places increasing pressure on natural land surfaces, reducing their permeability to stormwater. Consequently, surface runoff intensifies, overwhelming drainage systems and causing flash flooding with severe economic and social consequences [2,3]. The widespread use of impervious pavements exacerbates these issues by promoting waterlogging and water pollution during heavy rainfall, while simultaneously decreasing evaporation and contributing to the formation of urban heat islands [4,5].

To mitigate these impacts, urban planners and researchers have emphasized the need for efficient stormwater management systems. Permeable pavements play a critical role in controlling surface water runoff and supporting sustainable urban drainage systems [6,7]. These systems are especially beneficial for areas with inadequate natural drainage, contaminated soils, or where groundwater protection is essential [8,9].

Cost-effective implementation is crucial in pavement construction, especially in developing regions [10–12]. Enhancing the permeability of pavement materials not only alleviates flooding but also improves resilience to environmental and biological stresses [13]. Among the various technologies developed, pervious concrete has attracted significant attention for its dual capacity to allow water infiltration and support structural loads [14].

Effective design of pervious concrete must consider multiple factors, including permeability [15], moisture content [16,17], water absorption [18], air void content [19], and mechanical properties such as compressive [20,21] and flexural strength [22,23]. Recent research has explored the substitution of conventional aggregates with alternative materials to identify optimal combinations that provide sufficient water permeability and mechanical durability [24–28].

Other approaches have focused on optimizing mix designs to improve permeability while maintaining structural integrity [29,30]. For example, incorporating natural and synthetic fibers has been shown to enhance both permeability and mechanical properties of pervious concrete [21,31]. Use of ultra-high-performance concrete (UHPC) with fibers has led to notable improvements in strength and durability [32], while modeling of moisture diffusion coefficients has helped optimize performance under varying environmental conditions [33].

Despite these advancements, a notable research gap remains in optimizing the internal void structure and overall performance of pervious concrete using affordable, locally sourced materials. Many studies rely on imported or industrially processed admixtures, limiting the practical applicability of their findings in regions with resource constraints. While some efforts have explored fibers and supplementary cementitious materials, their combined effects—particularly when using readily available pozzolans and cost-effective fibers—remain underexplored [34].

Recent studies have also reported successful use of polypropylene fibers and pozzolanic materials to improve the mechanical strength, permeability, and durability of permeable concrete [35–37]. Similarly, natural additives and recycled materials like rice husk ash and biomass aggregates have enhanced the sustainability and compressive strength of concrete [38–40]. In parallel, the application of machine learning algorithms to predict and optimize the properties of pervious and geopolymer concretes is growing, contributing to more efficient mix design and environmental assessment [41,42].

While permeable concrete is widely recognized for its role in sustainable urban drainage, few studies have explored the synergistic impact of locally available pozzolanic materials and polypropylene fibers on both hydraulic and mechanical properties [43–45]. Most existing research emphasizes industrially processed or imported admixtures, which can be costly and environmentally unsuitable for developing regions[46].

This study introduces a novel mix design that uniquely combines ceramic powder and calcium carbide residue—two abundant, low-cost pozzolanic materials—with polypropylene fibers.

The core innovation lies in leveraging these locally sourced materials to create a permeable concrete that is not only structurally durable and highly permeable but also economically and environmentally sustainable. By focusing on cost-effective materials readily available in developing regions, this research proposes a practical and scalable solution for urban flood management, infrastructure resilience, and sustainable development—an area that remains underexplored in the current literature.

In light of these considerations, this study presents a novel and practical approach to pervious concrete design, aiming to balance permeability, mechanical strength, and material sustainability. The paper's structure is as follows: Section 2 describes the materials, experimental procedures, and mix design methodology. Section 3 presents the results of permeability, compressive and flexural strength, porosity, and density tests. Section 4 offers a critical discussion of the findings, contextualized within current literature and practical applications. Finally, Section 5 concludes the study, highlighting its contributions and suggesting directions for future work, particularly in the areas of long-term performance, environmental assessment, and economic feasibility.

2. Methodology

This study followed a systematic approach to develop and evaluate pervious concrete mixtures incorporating locally available pozzolanic materials and polypropylene fibers. The methodology consisted of four main stages: (1) selection and testing of raw materials including aggregates, cement, pozzolans, and fibers; (2) formulation of multiple mix designs with varying proportions of ceramic powder, calcium carbide residue, and two aggregate types; (3) laboratory testing of the prepared concrete samples to assess mechanical and physical properties such as compressive strength, flexural strength, permeability, air void content, and density; and (4) statistical analysis to identify the optimal mix design. Various specimen geometries were used for specific tests, ensuring accurate and standard-compliant measurements. The overall methodological framework is illustrated in Fig. 1.

2.1. Materials

A comprehensive range of materials was utilized for the design and fabrication of the pervious concrete mixtures, including cement, aggregates, water, ceramic powder, calcium carbide residue, and polypropylene fibers. Each material was selected based on local availability, compliance with standards, and its functional performance in permeable concrete systems.

2.1.1. Cement

Type II Portland cement, manufactured by Shargh Mashhad Cement Company, was used as the primary binder. The chemical composition and physical characteristics of the cement comply with the requirements of ASTM C150 [47], as outlined in Table 1. The cement exhibited appropriate strength, fineness, and setting time, suitable for hydraulic applications in permeable pavements.

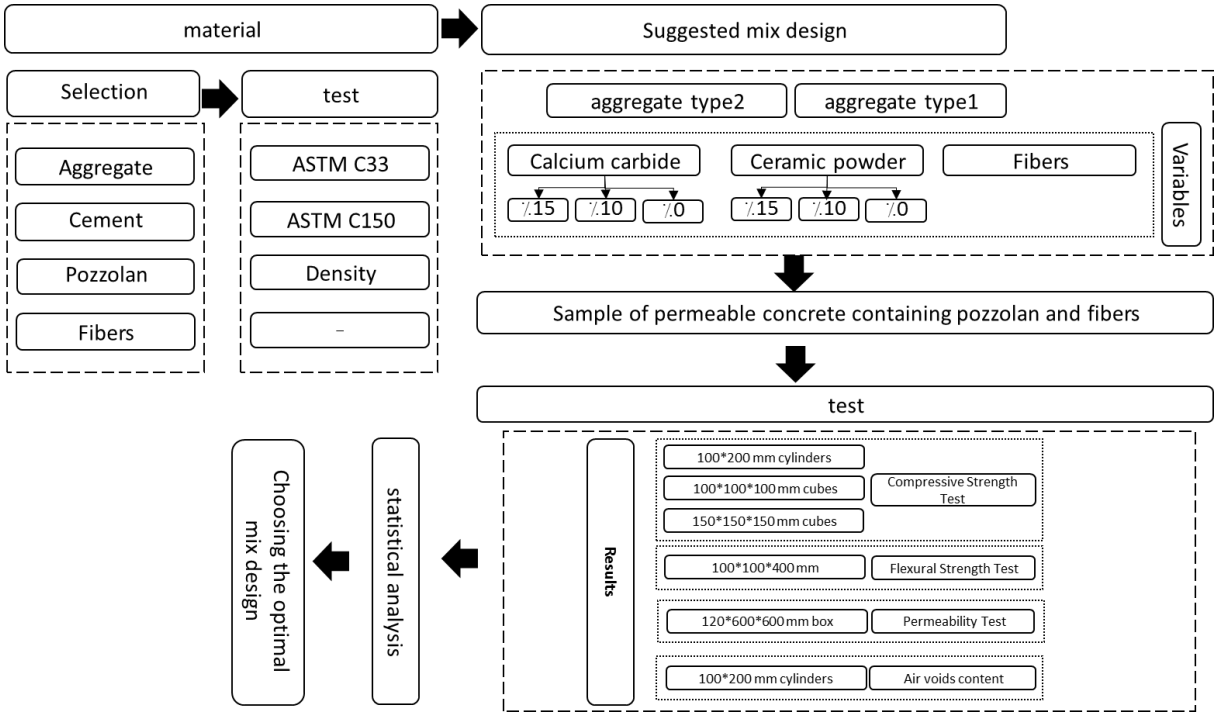

Fig. 1. Flowchart of the experimental methodology, including material selection, suggested mix design with variable components (ceramic powder, calcium carbide, fibers, and aggregates), sample preparation, and performance testing. The results were analyzed statistically to identify the optimal mix design based on permeability and mechanical properties.

Table 1. Chemical and physical properties of Type II Portland cement used in the mix (ASTM C150 compliant).

Property	Test Method	Result	ASTM C150 Requirement
Chemical Composition			
Silicon oxide (SiO_2), max %	ASTM C114	21	Min: 20
Aluminum oxide (Al_2O_3), max, %	ASTM C114	5.8	Max: 6
Ferric oxide (Fe_2O_3), max, %	ASTM C114	3.9	Max: 6
Calcium oxide (CaO), max %	ASTM C114	63.1	—
Magnesium oxide (MgO), max, %	ASTM C114	3.2	Max: 6
Sulfur trioxide (SO_3), max, %	ASTM C114	2.4	Max: 3
weight loss due to heat	ASTM C114	1.2	Max: 3
Insoluble residue	ASTM C114	0.25	Max: 1.5
Tricalcium silicate (C_3S) , max, %	ASTM C114	53.4	—
Dicalcium silicate (C_2S) , min, %	ASTM C114	19.9	—
Tricalcium aluminate (C_3A), max, %	ASTM C114	7.7	Max: 8
Chemical Composition			
Autoclave expansion, %	ASTM C151	0.04	Max 0.8
Compressive strength (3-day), Ib/in2	ASTM C109	2240	—
Compressive strength (7-day), Ib/in2	ASTM C109	2823	—
Compressive strength (28-day), Ib/in2	ASTM C109	4200	≥ 4000 (typical)
Density (g/cm³)	ASTM C188	3.14	—
Fineness, specific surface (m²/kg)	ASTM C204	290	Min 260
Setting time (initial), min	ASTM C191	185	Min 45
Setting time (final), min	ASTM C191	260	Max 375

2.1.2. Aggregates

Two types of natural coarse aggregates—Type 1 (medium-grained) and Type 2 (coarse-grained)—were sourced from quarries along the Mashhad-Kalat Road. Their gradation met the specifications of ASTM C33/C33M–13 [48]. The physical and mechanical properties, such as wear resistance, water absorption, and density, were characterized through standardized tests and are presented in Table 2.

Table 2. Physical properties of coarse aggregates used in the mix (Type 1: medium-grained, Type 2: coarse-grained).

Property	Test Method	Aggregate Type 1	Aggregate Type 2
Granulation type	—	C	B
Number of revolutions (rpm)	ASTM C131	500	500
Wear (Los Angeles Abrasion), %	ASTM C131/C131M	24	21
Sulfate resistance (Na_2SO_4), % loss	ASTM C88	0.9	1.0
Shape characteristics			
Elongation (%)	BS 812	2.3	35
Flakiness (%)	BS 812	9.0	12
Density and water absorption			
Bulk specific gravity (SSD), g/cm³	ASTM C127, C128	2.721	2.712
Apparent specific gravity, g/cm³	ASTM C127, C128	2.677	2.665
Water absorption, %	ASTM C127, C128	0.6	0.7
Unit weight			
Unit weight (dense), g/cm³	ASTM C29	1.57	1.60
Unit weight (loose), g/cm³	ASTM C29	1.43	1.47

Fig. 2 illustrates the particle size distribution curves for the two aggregate types, obtained through sieve analysis. Corresponding passing percentages for each sieve size are provided in Table 3, ensuring reproducibility of the mix designs.

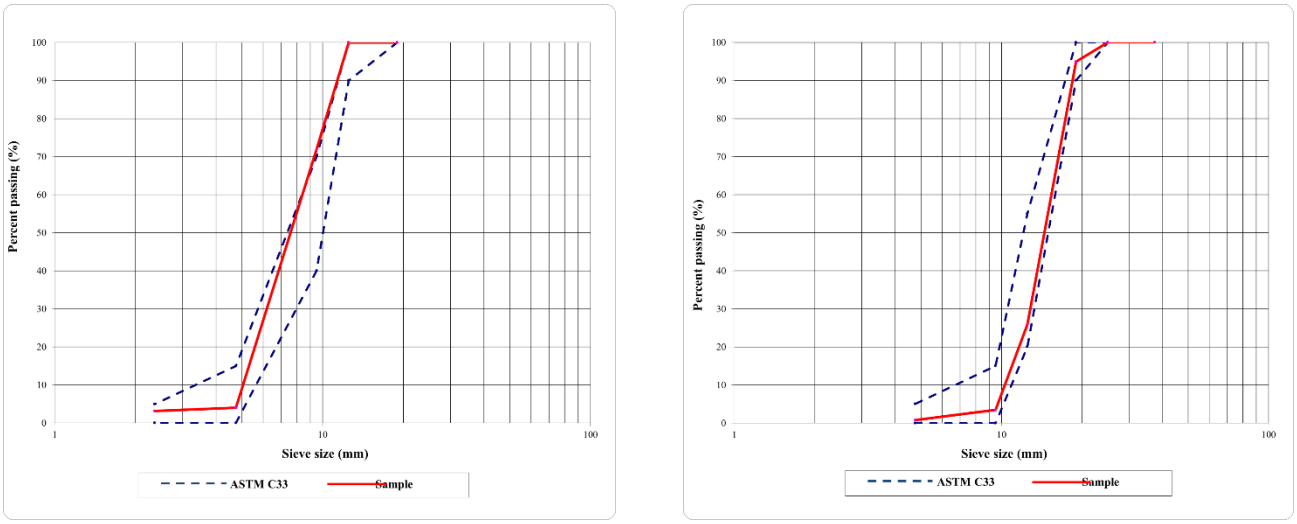

a b

Fig. 2. Particle size distribution curves for (a) Type 1 – medium-grained and (b) Type 2 – coarse-grained aggregates.

Table 3. Sieve analysis results for Type 1 (medium-grained) and Type 2 (coarse-grained) aggregates.

Sieve Size (mm)	% Passing (Type 1)	% Passing (Type 2)
12.5	100.0	100.0
9.5	95.2	89.1
4.75	62.3	47.6
2.36	35.8	25.7
1.18	18.9	12.4
0.60	9.1	5.6
0.30	3.7	2.1
0.15	1.4	0.7

2.1.3. Water

Potable water obtained from Mashhad City's municipal supply was used for all mixing and curing processes, ensuring consistency and compliance with standard water quality requirements for concrete production.

2.1.4. Pozzolanic materials

Two types of locally sourced pozzolanic materials were incorporated as partial cement replacements to improve sustainability and performance:

- Calcium carbide residue (CaC_2), a by-product obtained from the Acetylene Gas Company on the Mashhad-Kalat Road, was selected for its latent hydraulic properties.
- Ceramic powder, a fine industrial waste generated from tile manufacturing facilities in the industrial zones of Mashhad, was used as a reactive pozzolan. It reacts with calcium hydroxide during cement hydration to form additional calcium silicate hydrate (C–S–H), thereby enhancing the strength and durability of the cement.

2.1.5. Polypropylene fibers

Polypropylene fibers were employed as internal reinforcement to improve crack resistance and toughness while maintaining porosity. Due to the corrosion risks associated with conventional steel reinforcement in pervious systems, polypropylene fibers were chosen for their non-corrosive nature, cost-effectiveness, and ease of dispersion in the mix. The specifications of the fibers are listed in Table 4.

Table 4. Technical specifications of polypropylene fibers.

Parameter	Description
Manufacturer	MANA Fiber Ltd., Delijan, Iran
Raw Material	100% Virgin Polypropylene
Thickness	3 Denier
Fiber Length	12 mm
Diameter	40 μm
Tensile Strength	≥ 400 MPa
Melting Point	160–170 °C
Density	0.91 g/cm³
Shape	Monofilament
Surface	Coated for improved dispersion

2.2. Experimental setup and environmental conditions

All experimental procedures, including mixing, specimen preparation, and testing, were conducted following the outlined mix design methodology. Throughout these stages, environmental conditions were carefully controlled and maintained at a temperature of 21 ± 2°C and a relative humidity of 55 ± 5%, ensuring consistency in curing and testing conditions.

2.3. Equipment and apparatus

This section describes the major apparatus and instruments used in the experimental testing of pervious concrete properties.

2.3.1. Permeability testing setup

Permeability was assessed using a penetration ring conforming to ASTM C1781/C1781M–21 [49]. This ring is a watertight steel cylinder with a diameter of 300 mm and a height of 220 mm, open at both ends.

Its bottom edge is leveled to ensure uniform surface contact. Two reference lines, positioned 10 mm and 15 mm from the lower edge, are marked inside the ring to guide water depth and measurement consistency during infiltration testing.

2.3.2. Compressive strength testing setup

Compressive strength was measured using a CO160 hydraulic compressive testing machine (manufactured by Azmoon Co.), compliant with ASTM C39. The device has a maximum load capacity of 200 tons and features a digital display for force monitoring. Specimens were weighed using a precision Amput Electronic Scale (capacity: 5000 g, accuracy: 0.1 g). Before testing, all cylindrical specimens were surface-leveled using mechanical capping to ensure parallel ends, promoting uniform axial load distribution during failure.

During the test, cylindrical specimens were aligned within the machine's loading frame, and an axial load was applied at a constant rate of 0.5 kN/s until failure occurred. The maximum load recorded was taken as the ultimate compressive strength of the material.

2.3.3. Flexural strength testing setup

Flexural strength was evaluated using an STD1000 Universal Testing Machine, in compliance with ASTM C78 for concrete beam specimens. The apparatus includes a 100-ton load cell and adjustable third-point loading configuration. Beam specimens (100 × 100 × 400 mm) were tested with a span length of 300 mm and a loading rate of 0.2 mm/min. The failure load and corresponding deflections were recorded to calculate the modulus of rupture.

2.4. Mix design methodology

A total of eleven pervious concrete mixtures were developed based on the guidelines of ACI 211 for pervious concrete [50], with necessary adaptations to accommodate hydraulic performance, fiber reinforcement, and pozzolanic material integration. The mix design procedure accounted for both mechanical and permeability requirements relevant to urban drainage applications.

The binder system consisted of Portland cement (Type II) combined with locally available pozzolanic additives, specifically ceramic powder (Ce) and calcium carbide residue (Ca). Pozzolan replacement levels were systematically varied at 0%, 10%, and 15%, and one group incorporated a synergistic combination of 5% Ce and 5% Ca.

To ensure standardization, all mixes were prepared using the same type of cement, water-to-cement ratio, and identical curing conditions. A constant dosage of polypropylene fibers (1 kg per 60-liter batch, ~0.25% of the binder mass) was selected based on previous studies demonstrating that this dosage improves mechanical integrity and clogging resistance while maintaining good workability and fiber dispersion.

Preliminary trials were conducted to determine optimal aggregate ratios, ensuring adequate void structure, compressive strength, and hydraulic conductivity. The detailed mix proportions, including all cementitious and aggregate components, are listed in Table 5.

2.5. Mixing procedure and specimen casting

Concrete production began by dry mixing aggregates with polypropylene fibers, followed by the gradual addition of the cementitious materials (cement, ceramic powder, and calcium carbide residue). Finally, water was incrementally added to complete the mixing process using a 140-liter drum mixer (Azmoon Ltd.) operating at 35 rpm.

Table 5. Mix proportions of pervious concrete mixtures (per m³).

Mix ID	Description	Cement (kg/m³)	Ceramic Powder (Ce) (%)	Calcium Carbide (Ca) (%)	Fiber (kg/m³)	Water (kg/m³)	Aggregate Type 1 (kg/m³)	Aggregate Type 2 (kg/m³)
PC-1	A2 + Ca 5% + Ce 5% + Fiber	200	5	5	1	66.78	–	1678.2
PC-2	A1 + Ca 10% + Fiber	200	–	10	1	72.38	1692.04	–
PC-3	A1 + Ce 10% + Fiber	200	10	–	1	–	1703.5	–
PC-4	A1 (Control, no additives)	222.22	–	–	–	72.56	1701.43	–
PC-5	A2 (Control, no additives)	222.22	–	–	–	72.63	–	1708.1
PC-6	A2 + Ca 10% + Fiber	200	–	10	1	72.45	–	1698.7
PC-7	A2 + Ce 10% + Fiber	200	10	–	1	68.5	–	1702
PC-8	A2 + Ce 15%	200	15	–	–	73.14	–	1694.8
PC-9	A2 + Ca 15% + Fiber	200	–	15	1	67.2	–	1694.8
PC-10	A1 + Ce 15% + Fiber	200	15	–	1	71.1	1688.18	–
PC-11	A1 + Ca 15% + Fiber	200	–	15	1	73.1	1688.18	–

- A1 = Aggregate Type 1 (medium-grained)
- A2 = Aggregate Type 2 (coarse-grained)
- "–" indicates that the component was not used in that specific mix

Fresh concrete was cast into cylindrical molds (100 mm × 200 mm) for compressive and porosity testing, and into beam molds (100 mm × 100 mm × 400 mm) for flexural testing. Specimens were covered with plastic sheets for 24 hours post-casting to prevent moisture loss and were then cured in water until their designated testing age. The process of fabricating pervious concrete based on the mix design is illustrated in Fig. 3.

Fig. 3. Process of fabricating pervious concrete based on the designed mix procedure.

2.6. Testing procedures

2.6.1. Permeability test

The water infiltration capacity of the pervious concrete mixtures was evaluated according to the standard procedures outlined in ASTM C1781/C1781M–21 [49]. The test was designed to simulate realistic pavement conditions and quantify the infiltration rate (I) by measuring the infiltration time (T) and the mass of water (M) that passed through the specimen during testing.

A cylindrical steel infiltration ring, open at both ends and featuring an internal diameter of 305 mm, was used for the procedure. The ring was placed on the surface of a 600 mm × 600 mm × 120 mm slab specimen, ensuring watertight contact along the bottom edge. Water was poured into the ring to a predetermined height, and the time required for infiltration was recorded. The mass of infiltrated water was also measured for each test. The test configuration is shown in Fig. 4.

The infiltration rate was then calculated using the following equation:

$$I = \frac{K \times M}{(D^2 \times T)} \tag{1}$$

I denotes the infiltration rate, expressed in millimeters per hour (mm/h); M is the mass of water that infiltrated through the specimen, measured in kilograms (kg); D represents the internal diameter of the infiltration ring in millimeters (mm); T is the time required for water infiltration, measured in seconds (s); and K is the unit conversion constant, with a value of 4,583,666,000 in SI units (or 126,870 in inch-pound units).

This method provided a standardized and reproducible evaluation of surface permeability for each concrete mix.

Fig. 4. Permeability test setup using a steel infiltration ring placed on the surface of a pervious concrete slab.

2.6.2. Compressive strength test

The compressive strength of the pervious concrete mixtures was evaluated following ASTM C39/C39M [51], using cylindrical specimens with dimensions of 100 mm in diameter and 200 mm in height. The test was conducted at 28 days of curing, which is the standard age for assessing the structural performance of concrete.

Before testing, the end faces of the specimens were mechanically ground to produce smooth and parallel surfaces, ensuring uniform stress distribution during load application. This grinding method, instead of sulfur or neoprene capping, complies with ASTM C39 requirements for end preparation. The test setup and procedure are illustrated in Fig. 5.

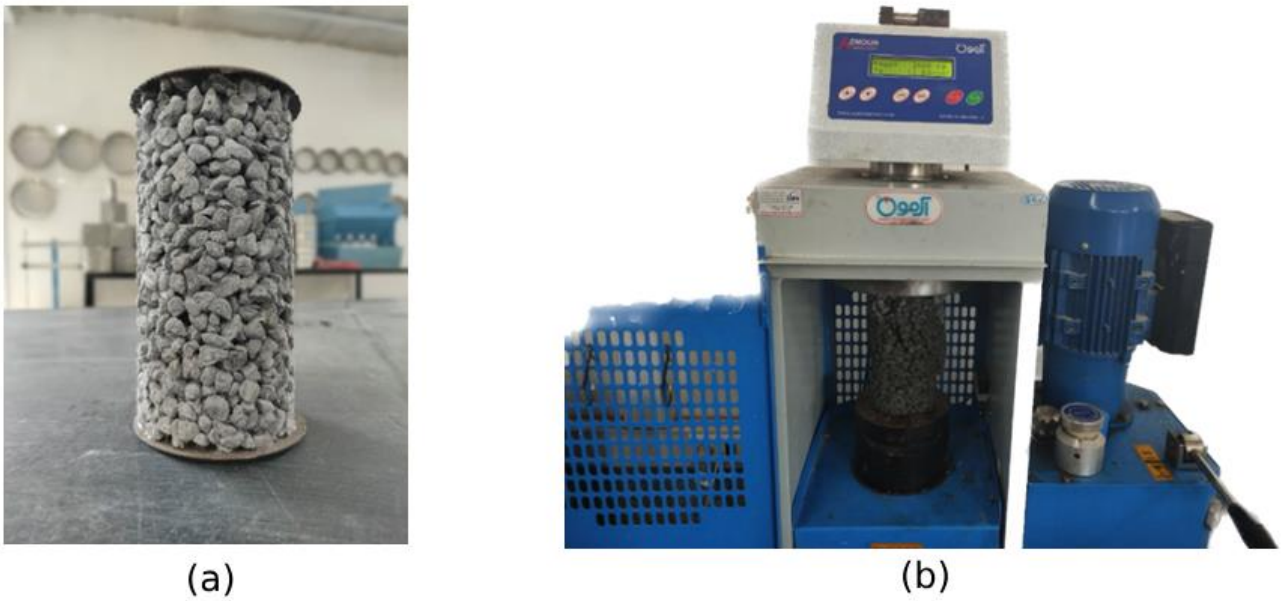

Fig. 5. Compressive strength testing of cylindrical specimen under axial loading at standard rate.

2.6.3. Flexural strength test

Flexural strength (modulus of rupture) was evaluated using ASTM C78/C78M-22 methodology [52]. Beam specimens (100 × 100 × 400 mm) were tested under third-point loading after 28 days of curing. The modulus of rupture (R) was calculated as:

$$R = \frac{P \times L}{b \times d^2} \tag{2}$$

R represents the modulus of rupture in megapascals (MPa); P is the maximum applied load at failure, measured in newtons (N); L denotes the span length between the supports in millimeters (mm); b is the average width of the specimen at the point of fracture (mm); and d is the average depth at the fracture location (mm).

2.6.4. Porosity and density test

The air void content was measured following ASTM C1754/C1754M – 12 [53]. Specimens were oven-dried at 38°C for 24 hours until a constant dry mass (A) was achieved. They were then submerged in water for 30 minutes, with agitation to release trapped air, and the submerged mass (B) was recorded.

Density and void content were calculated using the following formulas:

$$Density = \frac{K \times A}{D^2 \times L} \tag{3}$$

$$\text{Void Content} = (1 - \frac{A}{A - B}) \times 100 \tag{4}$$

K is a constant with a value of 1,273,240 in SI units; A represents the oven-dry mass of the specimen in grams (g); B is the submerged mass of the specimen in grams (g); D denotes the specimen diameter in millimeters (mm); and L is the specimen length in millimeters (mm).

Fig. 6 illustrates the setup and procedural steps involved in the porosity testing process, emphasizing the precise measurement techniques used to determine the air void content of the specimens.

Fig. 6. Porosity measurement using buoyancy method and submerged weight apparatus.

2.7. Data analysis

To evaluate the statistical significance of the influence of different mix designs on the mechanical and physical properties of pervious concrete, standard inferential statistical methods were employed. A one-way analysis of variance (ANOVA) was conducted to determine whether the observed differences among group means were statistically significant for key performance indicators, including permeability and flexural strength.

Following the ANOVA, Tukey's Honest Significant Difference (HSD) post-hoc test was applied to perform pairwise comparisons among the different concrete mixtures. This approach allowed for the identification of specific group differences while effectively controlling the family-wise error rate. The analysis included the computation of F-values, degrees of freedom (df), and p-values for each variable, as well as confidence intervals and mean differences derived from the Tukey HSD procedure.

The results of these statistical analyses are presented in the Results section through summary tables designed to facilitate clear interpretation and enhance reproducibility.

3. Results

3.1. Permeability performance

The permeability of each pervious concrete mixture was assessed as outlined in the Methodology section. Table 6 presents the test results, including the mass of infiltrated water, average infiltration time, and the calculated infiltration rate (I) for each mix design. These results reflect the influence of varying pozzolan content and fiber inclusion on the hydraulic performance of the concrete.

Table 6. Permeability test results for pervious concrete mixtures.

Mixed design	Water (kg)	Avg. Time (s)	Infiltration Rate, ***I*** (mm/h)
A2Ca.Ce 5%	18.25	6.38	140946.88
A1Ce. 10%	18.1	7.12	125259.84
A1Ca.Ce 10%	18.2	7.28	123183.71
A1	18.1	7.265	122759.82
A2	18	6.13	144685.60
A2Ca. 10%	18.2	7.925	113158.04
A2Ce. 10%	18.1	6.025	148024.91
A2Ce. 15%	18.15	10.295	86868.75
A2Ca. 15%	18.17	7.92	113042.83
A1Ce. 15%	18.12	11.19	79788.70
A2Ca.Ce 5%	18.14	10.59	84402.36

- *Mix Design*: Label for each specific pervious concrete formulation.
- *Water (kg)*: Mass of water infiltrated through the specimen.
- *Avg. Time (s):* Average time required for infiltration.
- *I (mm/h):* Calculated infiltration rate based on ASTM C1781/C1781M–21.

As shown in Table 6 and illustrated in Fig. 7, the permeability rates varied significantly, ranging from 79,788.70 mm/h to 148,024.91 mm/h across all mixtures. The base mixtures—A1 and A2—demonstrated infiltration rates of 122,759.82 mm/h and 144,685.60 mm/h, respectively.

Mixtures incorporating 15% pozzolan replacement (e.g., A2Ce 15%, A1Ce 15%) exhibited a statistically significant reduction in permeability ($p < 0.05$) compared to their respective base mixes. This reduction suggests that higher pozzolan content may partially obstruct the pore network or reduce effective void connectivity. In contrast, mixes containing 10% pozzolan replacement, such as A1Ce 10% and A1Ca.Ce 10%, demonstrated permeability values statistically comparable ($p > 0.05$) to the control group A1, indicating that moderate pozzolan incorporation can maintain effective water infiltration. Similarly, the A2Ca.Ce 5% mix—combining 5% ceramic powder and 5% calcium carbide residue—also showed permeability close to that of the A2 base mix, suggesting that a balanced dual-pozzolan approach can preserve hydraulic performance.

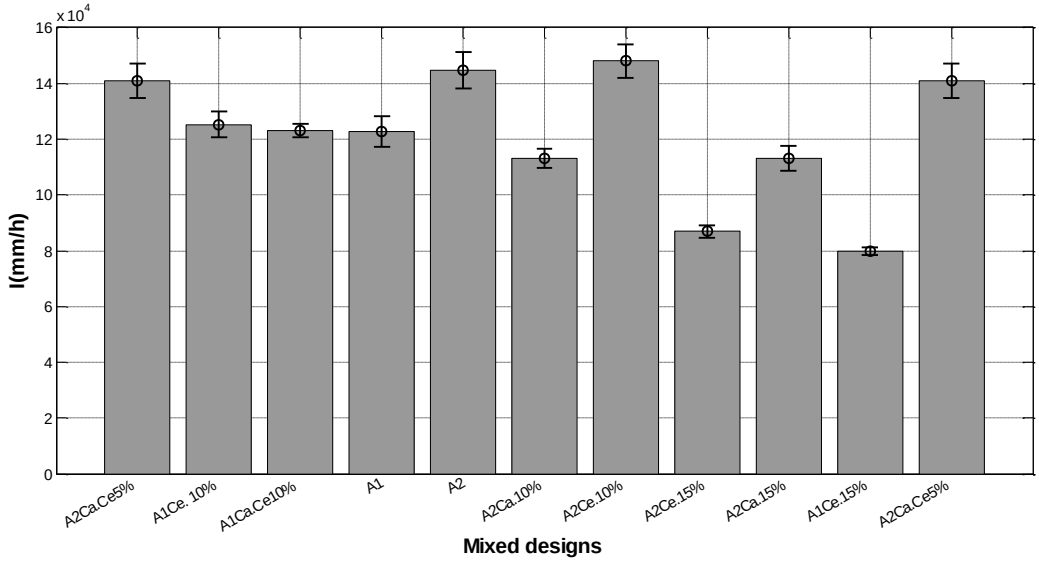

Fig. 7. Infiltration rates of pervious concrete mixtures with various pozzolan contents and aggregate types. Bars represent the mean infiltration rate values, and the error bars indicate the standard deviation based on multiple replicate measurements for each mix design.

3.2. Compressive strength performance

The compressive strength of each pervious concrete mix was evaluated at 7 and 28 days following ASTM C109. Table 7 presents the mean values and standard deviations for each mix design, highlighting the effects of pozzolanic materials and polypropylene fiber reinforcement on mechanical performance.

Table 7. Compressive strength results for pervious concrete mixes (Mean ± SD).

Mix Design	7-day Strength (MPa)	28-day Strength (MPa)
A2Ca.Ce 5%	10.2 ± 0.4	14.5 ± 0.6
A1Ce.10%	9.8 ± 0.5	13.2 ± 0.7
A1Ca.Ce 10%	10.1 ± 0.3	14.0 ± 0.5
A1	9.7 ± 0.4	12.8 ± 0.6
A2	10.5 ± 0.6	15.1 ± 0.7
A2Ca.10%	10.0 ± 0.5	13.9 ± 0.6
A2Ce.10%	9.6 ± 0.4	12.7 ± 0.5
A2Ce.15%	8.9 ± 0.3	11.5 ± 0.4
A2Ca.15%	9.5 ± 0.4	12.9 ± 0.5
A1Ce.15%	8.5 ± 0.3	11.0 ± 0.4
A2Ca.Ce 5%	10.3 ± 0.5	14.4 ± 0.6

The 28-day compressive strengths for all mixes exceeded the minimum threshold typically recommended for pervious concrete pavements, as indicated by the red dashed line in Fig. 8. Notably, the highest compressive strength was observed in the A2Ca.Ce 5% and A2Ca 10% mixtures, reaching 14.5 MPa and 13.9 MPa, respectively. These results suggest that moderate substitution of cement with calcium carbide residue and ceramic powder—either individually or in combination—can enhance compressive strength without compromising material performance.

In contrast, mixtures with higher pozzolan replacement levels (15%), such as A1Ce 15% and A2Ce 15% exhibited reduced strength values, indicating that excessive substitution may adversely affect the load-bearing capacity. The performance trend highlights the importance of optimizing pozzolan dosage to strike a balance between sustainability and mechanical performance.

Fig. 8 provides a graphical comparison of 28-day compressive strengths across all mix designs. The results demonstrate the mechanical benefit of incorporating optimized amounts of local pozzolanic materials and fiber reinforcement into pervious concrete.

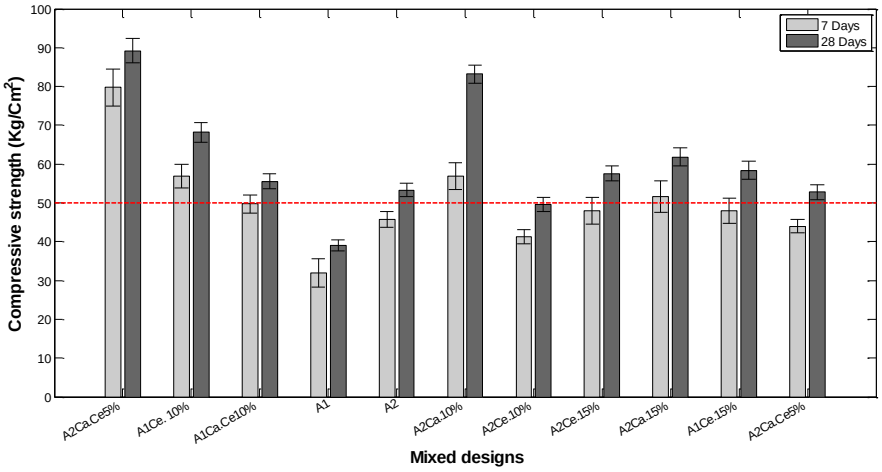

Fig. 8. Compressive strength of pervious concrete mixtures at 28 days. The red dashed line indicates the minimum strength requirement for pavement applications.

3.3. Flexural strength performance

Flexural strength testing was performed to evaluate the tensile performance of the pervious concrete mixtures under bending conditions, following the procedures outlined in ASTM C78/C78M. Beam specimens with dimensions of 100 × 100 × 400 mm were tested using a third-point loading configuration. The results are presented in Table 8, along with standard deviations to reflect variability among replicate samples.

Table 8. Flexural strength of pervious concrete mixes (Mean ± SD).

Mix Design	Flexural Strength (MPa)
A2Ca.Ce 5%	2.4 ± 0.1
A1Ce.10%	2.2 ± 0.1
A1Ca.Ce 10%	2.3 ± 0.1
A1	2.1 ± 0.1
A2	2.5 ± 0.2
A2Ca.10%	2.3 ± 0.1
A2Ce.10%	2.0 ± 0.1
A2Ce.15%	1.8 ± 0.1
A2Ca.15%	2.1 ± 0.1
A1Ce.15%	1.7 ± 0.1
A2Ca.Ce 5%	2.4 ± 0.1

As illustrated in Fig. 9, flexural strength varied noticeably across the different mix designs. Mixes incorporating 15% pozzolan replacement exhibited a significant improvement in flexural strength ($p < 0.05$) when compared to the control mixes (A1 and A2). Among these, the mix A2 achieved the highest average value at 2.5 MPa, while the 15% pozzolan mixes, such as A2Ca.15% and A2Ce.15%, also demonstrated performance exceeding baseline values.

In contrast, mixes with 10% pozzolan replacement—specifically A2Ca.Ce 5%, A1Ca.Ce 10%, and A1Ce.10%—achieved statistically similar flexural strength ($p > 0.05$) to the baseline designs, suggesting that moderate pozzolan content can maintain bending performance. However, A2Ce.10%, despite containing 10% pozzolan, exhibited a slight reduction in flexural strength compared to the control.

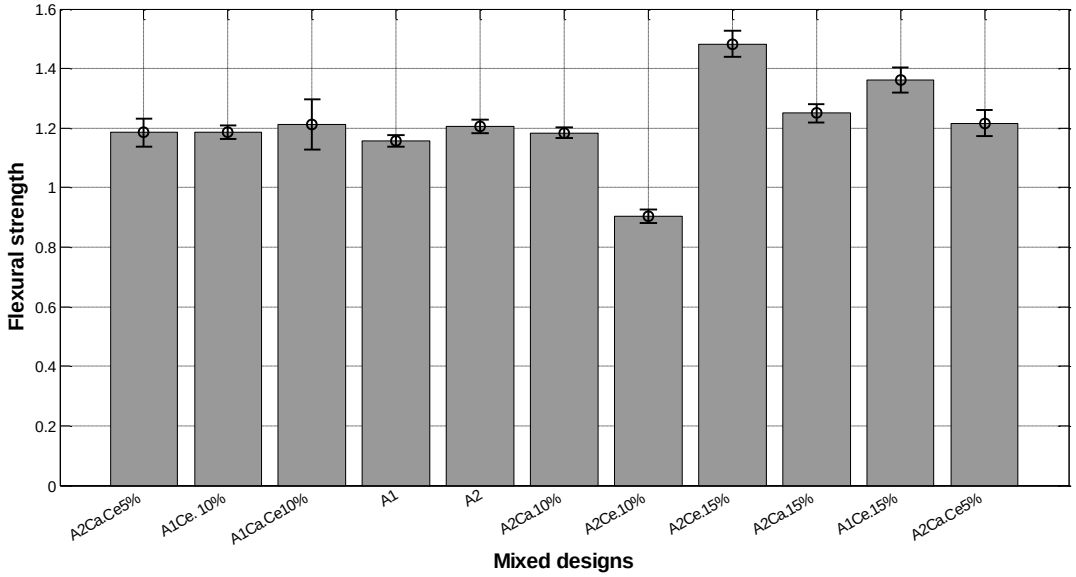

Fig. 9. Flexural strength of pervious concrete mixtures after 28 days of curing.

These findings indicate that while a higher pozzolan dosage can enhance flexural strength, the type and combination of pozzolanic materials, along with fiber integration, play a critical role in influencing mechanical behavior under flexural loading.

3.4. Failure pattern analysis

The failure modes observed during the compressive and flexural strength tests were documented through visual inspection to assess the structural behavior of each mix under load. Most concrete specimens containing 10% pozzolan replacement, such as A2Ca.Ce 5% and A1Ca.Ce 10%, exhibited a typical cone-shaped failure pattern under compression. This mode indicates a favorable stress distribution and stable fracture propagation, reflecting the material's ability to absorb and transfer loads efficiently.

In contrast, several mixes incorporating 15% pozzolan replacement, including A1Ce.15% and A2Ce.15%, predominantly experienced brittle failure modes, such as shear fractures or splitting failures. These types of failures indicate reduced energy dissipation and a tendency toward abrupt material breakdown, which is undesirable in pavement applications where gradual failure and post-crack stability are crucial for optimal performance.

These observations underscore the importance of optimizing pozzolanic content not only to enhance strength but also to promote ductile and predictable failure behavior. Achieving such a balance is essential for ensuring the long-term durability and safety of pervious concrete pavements under service loads.

3.5. Porosity and density performance

The air void content of the pervious concrete mixtures is illustrated in Fig. 10, with values ranging from 29.81% to 39.83% across the different mix designs. Each bar represents the mean value, accompanied by its standard deviation, which reflects the inherent variability in the experimental results.

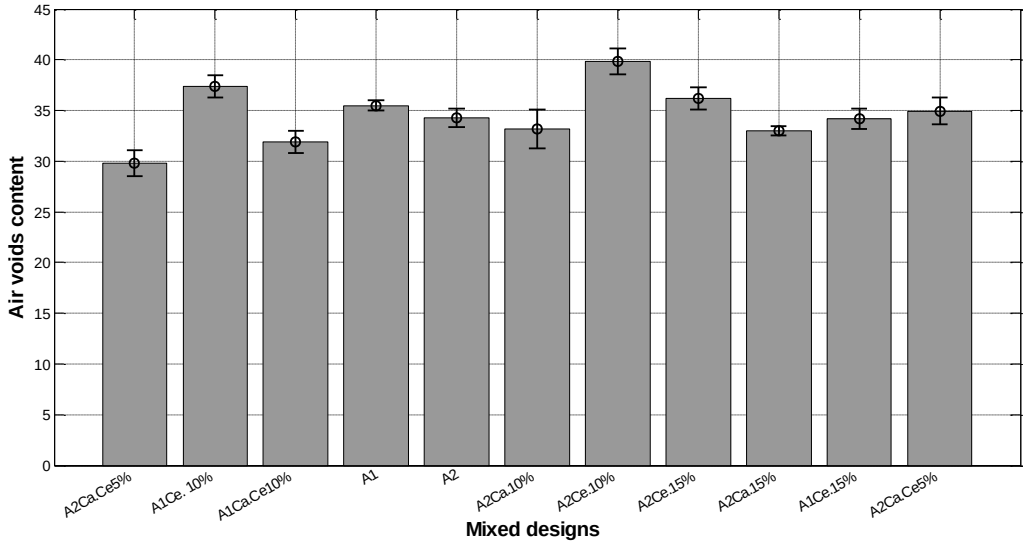

Fig. 10. Air void content of pervious concrete mixtures, including standard deviation bars.

Aggregate gradation and pozzolan dosage had a notable influence on porosity, although their interactive effects were not statistically significant. Among the baseline mixes, A2Ce 10% exhibited the highest porosity, reaching 39.83%, suggesting that higher ceramic pozzolan content may contribute to increased void formation. Conversely, designs with balanced or lower pozzolan content, particularly those using Type 1 aggregates (A1 series), generally demonstrated reduced air voids, indicating improved packing density.

Fig. 11 displays the bulk density values of the tested mixtures. The results reveal considerable variation, primarily influenced by the mix design, pozzolan content, and aggregate type. The highest density was recorded in A2Ca.Ce 5%, with a value of 1798.81 kg/m³, indicating a relatively dense and compact structure. In contrast, the lowest density was observed in A2Ce 10%, measured at 1592.26 kg/m³, consistent with its high air void content.

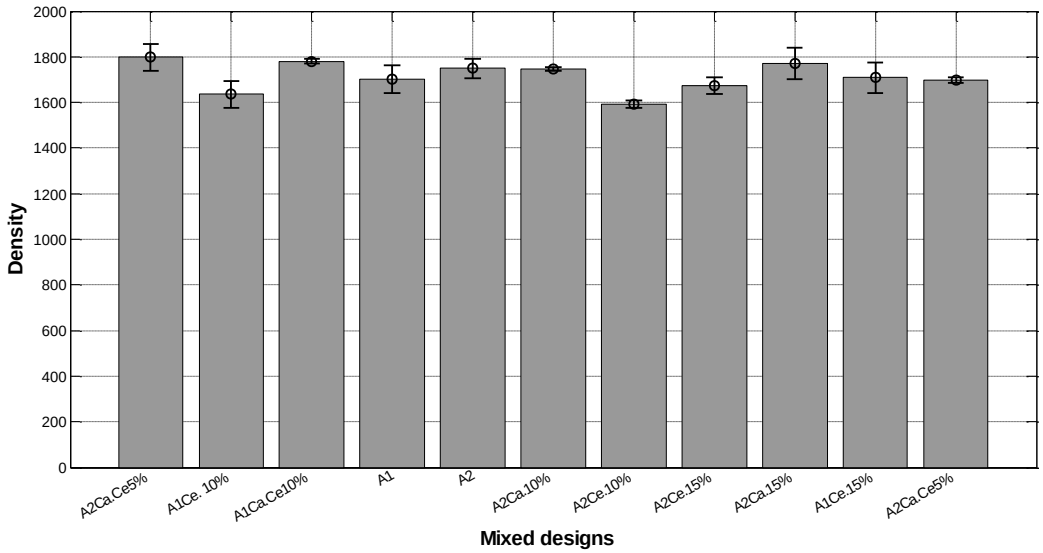

Fig. 11. Bulk density of pervious concrete mixtures across different mix designs.

These trends reinforce the inverse relationship between porosity and density, underscoring the need to balance these properties to ensure adequate mechanical strength while preserving the permeability of pervious concrete.

4. Discussion

This study presents a novel approach to the mix design of pervious concrete, aiming to enhance its performance in sustainable urban stormwater management. By integrating locally available pozzolanic materials and polypropylene fibers, the research successfully balances permeability enhancement with mechanical performance, contributing to both environmental and structural objectives.

The incorporation of supplementary cementitious materials aligns with previous findings on sustainable construction practices [54], reinforcing the importance of tailoring mix designs to meet specific performance requirements [55,56]. The results demonstrate a trade-off between permeability and mechanical strength. For instance, the A2Ce 10% mix, which included a 10% replacement with ceramic powder, exhibited one of the highest permeability and porosity values—features desirable for stormwater infiltration. However, this gain in permeability was accompanied by a reduction in flexural strength, highlighting the need to balance performance parameters according to the intended application.

Among all tested mixes, A2Ca.Ce 5% emerged as a well-balanced formulation. It achieved enhanced permeability while maintaining compressive strength and flexural performance comparable to the control mixes. Furthermore, its lower porosity and higher density values suggest better structural integrity. This composition offers a practical compromise for field applications where trade-offs between mechanical and hydraulic properties are acceptable within specified design tolerances.

According to ACI 522R-10 guidelines [57], typical permeability values for pervious concrete range from 2,000 to 20,000 mm/h, depending on mix composition, compaction, and porosity levels [50]. The substantially higher infiltration rates observed in this study—reaching up to 148,024.91 mm/h—highlight the exceptional drainage performance of the proposed mixes. This enhancement is attributed to the optimized aggregate gradation, well-structured void network, and the synergistic use of local pozzolanic materials and polypropylene fibers, which effectively preserved the pervious structure without significant clogging. The observation that 15% pozzolan replacement did not lead to significant permeability improvements warrants further investigation. These mixes may still offer benefits in terms of durability, resistance to chemical attack, or economic and environmental advantages, such as lower embodied carbon. Additionally, the role of polypropylene fibers merits further exploration, particularly concerning their effects on crack control, erosion resistance, and long-term mechanical performance under repeated loading.

Given the increasing focus on environmental sustainability, it is essential to consider the mechanical and structural performance, as well as the water consumption and permeability characteristics, of the developed mixes. The amount of water used for each mix design remained consistent, ranging from 18.0 to 18.25 kilograms. However, notable variations were observed in infiltration times and rates. For example, the A2Ce.10% mix had the shortest infiltration time (6.025 seconds) and the highest infiltration rate (148,024.91 mm/h), indicating superior permeability performance. Conversely, the A1Ce.15% mix had the longest infiltration time (11.19 seconds) and lowest infiltration rate (79,788.70 mm/h), indicating reduced porosity or blockage within the matrix. These differences underscore the significant influence of pozzolanic content and type on the hydraulic behavior of the mixes. Such data is valuable for urban applications, as rapid water infiltration is essential for reducing surface runoff and mitigating flood risks. Therefore,

evaluating water usage and permeability parameters, in addition to mechanical properties, provides a more comprehensive understanding of the environmental performance of the mixes.

This research also aligns with broader trends in sustainable construction, where innovations in materials science—such as the use of high-volume fly ash concrete [58,59], alternative water sources [60], and nano-silica additives [61]—demonstrate the potential to enhance both environmental and mechanical performance. Similarly, advancements in strengthening techniques, such as Basalt Fiber Reinforced Polymers (BFRP), have shown promise in enhancing structural elements like T-beams under flexural stress [62,63]. These developments collectively support the notion that sustainable material design must consider a range of structural and environmental performance metrics [64].

Despite the promising results of this study, its limitations must be acknowledged. The experiments were conducted under controlled laboratory conditions, with a focus on short-term performance. In real-world applications, pervious concrete is subjected to a variety of environmental stressors, such as freeze-thaw cycles, ultraviolet radiation, deicing salts, and clogging from organic debris [65,66]. These factors can significantly influence the long-term performance of the material. Therefore, future studies should incorporate field trials and accelerated durability testing to validate the laboratory findings under realistic service conditions.

A critical next step involves conducting a Life Cycle Assessment (LCA) to evaluate the environmental footprint of the proposed mix designs from raw material extraction through to end-of-life disposal [67,68]. Such an assessment would quantify the sustainability benefits of incorporating locally sourced pozzolans and synthetic fibers [69], while also considering impacts such as reduced stormwater runoff, maintenance requirements, and energy consumption. Moreover, calculating the carbon footprint associated with the proposed mix design compared to conventional alternatives could offer insight into its contribution to climate change mitigation efforts [70,71].

To facilitate real-world implementation, a comprehensive life-cycle cost analysis (LCCA) is also necessary. This analysis should account for material costs, including the availability and processing of local pozzolans, as well as potential savings from improved durability, reduced maintenance, and faster installation processes [72,73]. Economic viability will be a key factor in determining the practical adoption of these formulations. Future research should thus explore the cost-benefit dynamics of the proposed mixes in comparison to traditional pervious concrete systems, considering both environmental and economic performance over time [74].

Lastly, the adaptability of these optimized mixes to different climatic conditions and traffic loading scenarios should be evaluated to extend the applicability of findings across diverse urban contexts. By addressing long-term performance, economic feasibility, and regional adaptability, this line of research can significantly advance the development of pervious concrete as a high-performance, sustainable solution for modern urban infrastructure.

5. Conclusions

This study examined the effect of pozzolanic replacements and the incorporation of polypropylene fibers on the performance characteristics of pervious concrete. The findings demonstrated that permeability values ranged from approximately 79,789 to 148,025 mm/h, with the A2Ca.Ce 5% mix achieves the highest infiltration rate. Mixes containing 10% pozzolan substitution-maintained permeability levels statistically similar to the baseline ($p > 0.05$), indicating their suitability for maintaining hydraulic functionality. Compressive strength results exceeded the minimum threshold required for pavement applications across

all mixtures, with the highest value recorded at 89.18 kg/cm² in the A2Ca.Ce 5% mix. Flexural strength was significantly enhanced ($p < 0.05$) in the 15% pozzolan replacement designs; however, a notable exception was observed in the A2Ce 10% mix, which exhibited reduced flexural strength relative to the control.

The air void content varied between 29.81% and 39.83%, influenced by both pozzolan dosage and aggregate type, while the density values ranged from 1,592 to 1,799 kg/m³, notably for the A2Ca.Ce 5% mixture not only exhibited the highest density but also demonstrated a favorable balance across all key performance metrics. Taken together, these results identify A2Ca.Ce 5% as a promising mix design, offering an optimal combination of high permeability, mechanical strength, and structural integrity. This balanced performance highlights its potential for practical application in sustainable pervious concrete pavements, particularly in urban environments requiring both efficient stormwater management and long-term durability.

Funding

This research received no external funding.

Conflicts of interest

The authors declare that they have no conflict of interest.

Authors contribution statement

Mahmoud Taghdisi: Conceptualization, methodology development, experimental design, research execution, and manuscript writing.

Kazem Esmaili: Conceptualization, methodology development, resource provision, supervision, research execution, and manuscript writing.

Saeed Reza Khodashenas: Manuscript review, validation of results, data visualization, and writing.

Seyed Ali Ziaei: Manuscript review, resource management, research participation, and writing. Saeed Fatemi: Manuscript review, resource management, research participation, and writing.

6. References

[1] Hannah R, Max R. Urbanization. Our World Data 2018.

[2] Fabio R, Andrea P, Maria Nicolina R, Antonio L. Assessment of stormwater runoff management practices and BMPs under soil sealing: A study case in a peri-urban watershed of the metropolitan area of Rome (Italy). J Environ Manage 2017;201:6–18. https://doi.org/10.1016/j.jenvman.2017.06.024.

[3] Giuseppina G, Andrea G, Patrizia P, Giandomenico S, Andrea V. A distributed real-time approach for mitigating CSO and flooding in urban drainage systems. J Netw Comput Appl 2017;78:30–42. https://doi.org/10.1016/j.jnca.2016.11.004.

[4] Ji Hun P, Young Uk K, Jisoo J, Seunghwan W, Seong Jin C, Sumin K. Effect of eco-friendly pervious concrete with amorphous metallic fiber on evaporative cooling performance. J Environ Manage 2021;297:113269. https://doi.org/10.1016/j.jenvman.2021.113269.

[5] Ernest O. N, Alan P. N, Stephen J. C, Fredrick U. M. Stormwater harvesting for irrigation purposes: An investigation of chemical quality of water recycled in pervious pavement system. J Environ Manage 2015;147:246–56. https://doi.org/10.1016/j.jenvman.2014.08.020.

[6] J. S, X. K, G. Y, V. R. Filtration and clogging of permeable pavement loaded by urban drainage. Water Res 2012;46:6763–74. https://doi.org/10.1016/j.watres.2011.10.018.

[7] Masoud K, Hui L, John T. H, Xiao L. Application of permeable pavements in highways for stormwater runoff management and pollution prevention: California research experiences. Int J Transp Sci Technol 2019;8:358–72. https://doi.org/10.1016/j.ijtst.2019.01.001.

[8] Jennifer D, Andrea B, Tim VS. Hydrologic Performance of Three Partial-Infiltration Permeable Pavements in a Cold Climate over Low Permeability Soil. J Hydrol Eng 2014;19:04014016. https://doi.org/10.1061/(ASCE)HE.1943-5584.0000943.

[9] Adam C. Performance of Hydromedia Pervious Concrete Pavement Subjected to Urban Traffic Loads in Ontario. n.d.

[10] Tarunbir S, Rafat S, Shruti S. Effectiveness of using Metakaolin and fly ash as supplementary cementitious materials in pervious concrete. Eur J Environ Civ Eng n.d.;26:7359–82. https://doi.org/10.1080/19648189.2021.1988715.

[11] John T. K, Joseph Dan S. Low-Cost Techniques for Improving the Surface Durability of Pervious Concrete. Transp Res Rec n.d.:83–9. https://doi.org/10.3141/2342-10.

[12] Xiaodan C, Hao W, Husam N, Giri V, John H. Evaluating engineering properties and environmental impact of pervious concrete with fly ash and slag. J Clean Prod n.d.;237:117714. https://doi.org/10.1016/j.jclepro.2019.117714.

[13] Sara P-M, Ignacio A-D, Carmen H-C, Francisco V-M, Miguel M, Ignacio E-B, et al. The role of monitoring sustainable drainage systems for promoting transition towards regenerative urban built environments: a case study in the Valencian region, Spain. J Clean Prod 2017;163:S113–24. https://doi.org/10.1016/j.jclepro.2016.05.153.

[14] L. C, T. F. F. Evaluation of surface infiltration performance of permeable pavements. J Environ Manage 2019;238:136–43. https://doi.org/10.1016/j.jenvman.2019.02.119.

[15] Effect of clogging and cleaning on the permeability of pervious block pavements: International Journal of Pavement Engineering: Vol 23, No 9 n.d.

[16] Md Habibullah B, Shriful I, Joe G, Jeffrey L, Alexander S. Application of Time Domain Reflectometry Method in Monitoring State Parameters of Subgrade Soil in Pavement. J Transp Eng Part B Pavements 2020;146:04020021. https://doi.org/10.1061/JPEODX.0000172.

[17] Sayedmasoud M, Majid G, Eshan V. D. A system dynamics framework for mechanistic analysis of flexible pavement systems under moisture variations. Transp Geotech 2021;30:100619. https://doi.org/10.1016/j.trgeo.2021.100619.

[18] P S, M H, BH N, I A. Laboratory comparison of roller-compacted concrete and ordinary vibrated concrete for pavement structures. GRADEVINAR n.d.;72:127–37. https://doi.org/10.14256/JCE.2572.2018.

[19] Alalea K, Jasmine M. D, Hong S. W, Christopher R. C. Structural and hydrological design of permeable concrete pavements. Case Stud Constr Mater 2021;15:e00564. https://doi.org/10.1016/j.cscm.2021.e00564.

[20] Weichung Y, Jiang Jhy C. The influences of cement type and curing condition on properties of pervious concrete made with electric arc furnace slag as aggregates. Constr Build Mater 2019;197:813–20. https://doi.org/10.1016/j.conbuildmat.2018.08.178.

[21] Savithri S. K, U. Lohith K, Naveen D. Porous concrete with optimum fine aggregate and fibre for improved strength. Adv Concr Constr 2019;8:305–9.

[22] FRAM C, BS S, H R, RA Y. Advanced Properties of Continuously Graded Pervious Concrete for Rigid Pavement Base Layer. Int J Eng Technol Innov n.d.;9:91–107.

[23] AK C, KP B. Investigation on Flexural Strength and Stiffness of Pervious Concrete for Pavement Applications. Adv Civ Eng Mater n.d.;7:223–42. https://doi.org/10.1520/ACEM20170015.

[24] Ebenezer Y, Pablo T, Daniel J-E, Gilberto Garcia DA, Carlos T. The Effect of Untreated Dura-Palm Kernel Shells as Coarse Aggregate in Lightweight Pervious Concrete for Flood Mitigation. BUILDINGS n.d.;13:1588. https://doi.org/10.3390/buildings13071588.

[25] Kwabena B, Morteza K. Influence of Calcined Clay Pozzolan and Aggregate Size on the Mechanical and Durability Properties of Pervious Concrete. J Compos Sci n.d.;7:182. https://doi.org/10.3390/jcs7050182.

[26] Guoyang L, Pengfei L, Yuhong W, Sabine F, Dawei W, Markus O. Development of a sustainable pervious pavement material using recycled ceramic aggregate and bio-based polyurethane binder. J Clean Prod n.d.;220:1052–60. https://doi.org/10.1016/j.jclepro.2019.02.184.

[27] Mudasir N, Kanish K, S. P. S. Strength, durability and microstructural investigations on pervious concrete made with fly ash and silica fume as supplementary cementitious materials. J Build Eng 2023;69:106275. https://doi.org/10.1016/j.jobe.2023.106275.

[28] Desmond E. E. E, Joseph O. O. U, Obeten Nicholas O, Zubair Ahmed M, George Uwadiegwu A, Abdalrhman M. Scheffe's Simplex Optimization of Flexural Strength of Quarry Dust and Sawdust Ash Pervious Concrete for Sustainable Pavement Construction. Materials (Basel) n.d.;16:598. https://doi.org/10.3390/ma16020598.

[29] J. X, C. J, J. A, J. P. Mix design and physical and mechanical properties of pervious concretes. Mater Constr n.d.;72:e297. https://doi.org/10.3989/mc.2022.292722.

[30] M. S. M. L, K. K. H, A. H. J, E. M, P. K. M. Self-Compacting Pervious Concrete Mix Design for Permeable Concrete Soakaway Rings. Adv Civ Eng Mater n.d.;7:340–52. https://doi.org/10.1520/ACEM20170153.

[31] Ming-Gin L, Wei-Chien W, Yung-Chih W, Yi-Cheng H, Yung-Chih L. Mechanical Properties of High-Strength Pervious Concrete with Steel Fiber or Glass Fiber. BUILDINGS n.d.;12:620. https://doi.org/10.3390/buildings12050620.

[32] Cong Z, Jianqun W, Xudong S, Lifeng L, Junbo S, Xiangyu W. The feasibility of using ultra-high performance concrete (UHPC) to strengthen RC beams in torsion. J Mater Res Technol 2023;24:9961–83. https://doi.org/10.1016/j.jmrt.2023.05.185.

[33] Fengbin Z, Wenhao L, Ying H, Lepeng H, Zhuolin X, Jun Y, et al. Moisture Diffusion Coefficient of Concrete under Different Conditions. Buildings n.d.;13:2421. https://doi.org/10.3390/buildings13102421.

[34] Lin C, Zhonghao C, Zhuolin X, Lilong W, Jianmin H, Lepeng H, et al. Recent developments on natural fiber concrete: A review of properties, sustainability, applications, barriers, and opportunities. Dev Built Environ 2023;16:100255. https://doi.org/10.1016/j.dibe.2023.100255.

[35] Salami BA, Bahraq AA, Haq MM ul, Ojelade OA, Taiwo R, Wahab S, et al. Polymer-enhanced concrete: A comprehensive review of innovations and pathways for resilient and sustainable materials. Next Mater 2024;4:100225. https://doi.org/https://doi.org/10.1016/j.nxmate.2024.100225.

[36] Khan R, Siddiqui AR, Akhtar MN. Sustainable concrete solutions for green infrastructure development: A review. J Sustain Constr Mater Technol 2025;10:108–41. https://doi.org/10.47481/jscmt.1667793.

[37] Bilal H, Gao X, Cavaleri L, Khan A, Ren M. Mechanical, Durability, and Microstructure Characterization of Pervious Concrete Incorporating Polypropylene Fibers and Fly Ash/Silica Fume. J Compos Sci 2024;8. https://doi.org/10.3390/jcs8110456.

[38] Onyelowe KC, Ebid AM, Mahdi HA, Riofrio A, Eidgahee DR, Baykara H, et al. Optimal Compressive Strength of RHA Ultra-High-Performance Lightweight Concrete (UHPLC) and Its Environmental Performance Using Life Cycle Assessment. Civ Eng J 2022;8:2391–410. https://doi.org/10.28991/CEJ-2022-08-11-03.

[39] Onyelowe KC, Kontoni DPN, Oyewole S, Apugo-Nwosu T, Nasrollahpour S, Soleymani A, et al. Compressive strength optimization and life cycle assessment of geopolymer concrete using machine learning techniques. E3SWC 2023;436:08009. https://doi.org/10.1051/E3SCONF/202343608009.

[40] Yosefi A, Jahangir H. The Influence of Natural Additives on Mechanical Properties of Concrete Specimens: A Review. | ۲۰–۵:۱۱;۲۰۲۳ | نشریه عمران و پروژه. https://doi.org/10.22034/cpj.2023.398231.1200.

[41] Sathiparan N, Jeyananthan P, Subramaniam DN. A machine learning approach to predicting pervious concrete properties: a review. Innov Infrastruct Solut 2025;10:1–43. https://doi.org/10.1007/S41062-024-01829-3/METRICS.

[42] Mhaya AM, Shahidan S, Mohd Zuki SS, Hakim SJS, Wan Ibrahim MH, Mohammad Azmi MA, et al. Modified pervious concrete containing biomass aggregate: Sustainability and environmental benefits. Ain Shams Eng J 2025;16:103324. https://doi.org/10.1016/J.ASEJ.2025.103324.

[43] Akbulut ZF, Kuzielová E, Tawfik TA, Smarzewski P, Guler S. Synergistic Effects of Polypropylene Fibers and Silica Fume on Structural Lightweight Concrete: Analysis of Workability, Thermal Conductivity, and Strength Properties. Mater 2024, Vol 17, Page 5042 2024;17:5042. https://doi.org/10.3390/MA17205042.

[44] Boomibalan S, Isleem HF, Swaminathan P, Rameshkumar D, Kadarkarai A. Experimental investigations on mechanical performance, synergy assessment, and microstructure of pozzolanic and non-pozzolanic hybrid steel fiber reinforced concrete. Struct Concr 2025;26:1498–519. https://doi.org/10.1002/SUCO.202400693;REQUESTEDJOURNAL:JOURNAL:17517648;WGROUP:STRING:PUBLICATION.

[45] Wang Y, Zhang J, Du G, Li Y. Synergistic effects of polypropylene fiber and basalt fiber on the mechanical properties of concrete incorporating fly ash ceramsite after freeze-thaw cycles. J Build Eng 2024;91:109593. https://doi.org/10.1016/J.JOBE.2024.109593.

[46] Althaqafi E, Ali T, Qureshi MZ, Islam S, Ahmed H, Ajwad A, et al. Evaluating the combined effect of sugarcane bagasse ash, metakaolin, and polypropylene fibers in sustainable construction. Sci Rep 2024;14:1–17. https://doi.org/10.1038/S41598-024-76360-7;SUBJMETA=166,639,766;KWRD=ENGINEERING,PHYSICS.

[47] Standard Specification for Portland Cement n.d.

[48] Specification for Concrete Aggregates. n.d.

[49] Standard Test Method for Surface Infiltration Rate of Permeable Unit Pavement Systems n.d. https://doi.org/10.1520/C1781_C1781M–13.

[50] Gene Daniel D. Factors influencing concrete workability. ASTM Spec Tech Publ 2006;169 D-STP:59–72. https://doi.org/10.1520/stp36407s.

[51] Standard Test Method for Compressive Strength of Cylindrical Concrete Specimens n.d.

[52] Test Method for Flexural Strength of Concrete (Using Simple Beam with Third-Point Loading). n.d.

[53] Standard Test Method for Density and Void Content of Hardened Pervious Concrete n.d.

[54] Chittaranjan B. N. Experimental and numerical study on reinforced concrete deep beam in shear with crimped steel fiber. Innov Infrastruct Solut n.d.;7:41. https://doi.org/10.1007/s41062-021-00638-2.

[55] Chittaranjan B. N. Experimental and numerical investigation on compressive and flexural behavior of structural steel tubular beams strengthened with AFRP composites. J King Saud Univ - Eng Sci 2021;33:88–94. https://doi.org/10.1016/j.jksues.2020.02.001.

[56] Nilesh Z, Shantanu P, Chittaranjan N. Use of fly ash cenosphere in the construction Industry: A review. Mater Today Proc 2022;62:2185–90. https://doi.org/10.1016/j.matpr.2022.03.362.

[57] American Concrete Institute. ACI 522 R10 Reported by ACI Committee 522 Report on Pervious Concrete (Reapproved 2011). ACI Commitee 522 2010:1–08.

[58] N. R, M. S. R. Strength characteristics of concrete made with copper slag and fly-ash. Mater Today Proc 2022;60:738–45. https://doi.org/10.1016/j.matpr.2022.02.337.

[59] Gunavant K. K, Chittaranjan B. N, Sunil B. T. Optimization of sustainable high-strength–high-volume fly ash concrete with and without steel fiber using Taguchi method and multi-regression analysis. Innov Infrastruct Solut 2021;6:102. https://doi.org/10.1007/s41062-021-00472-6.

[60] A P, C N, Chittaranjan N. An Experimental Study on Effect of Pharmaceutical Industrial Waste Water on Compressive Strength of Concrete. Int J Innov Res Sci Eng Technol 2021;10:5. https://doi.org/10.15680/IJIRSET.2021.1008038.

[61] Chittaranjan B. N, Pratik P. T, Umesh T. J, Nitin A. J, Samadhan G. M. Effect of SiO2 and ZnO Nano-Composites on Mechanical and Chemical Properties of Modified Concrete. Iran J Sci Technol Trans Civ Eng 2022;46:1237–47. https://doi.org/10.1007/s40996-021-00694-9.

[62] Chittaranjan B. N, Giridhar N. N, Harshwardhan R. S. Structural and cracking behaviour of RC T-beams strengthened with BFRP sheets by experimental and analytical investigation. J King Saud Univ - Eng Sci 2022;34:398–405. https://doi.org/10.1016/j.jksues.2021.01.001.

[63] Umesh J, Anil J, Chittaranjan N. Behaviour of Ternary Blended Cement in M40 Grade of Concrete 2022;9.

[64] Nagesh T. S, Chittaranjan B. N, Sunil B. T, Gunavant K. K. Optimization of Self-cured High-Strength Concrete by Experimental and Grey Taguchi Modelling. Iran J Sci Technol Trans Civ Eng 2022;46:4313–26. https://doi.org/10.1007/s40996-022-00897-8.

[65] Pengfei L, Haoyu W, Ding N, Duoyin W, Chengzhi W. A method to analyze the long-term durability performance of underground reinforced concrete culvert structures under coupled mechanical and environmental loads. J Intell Constr 2023;1. https://doi.org/10.26599/JIC.2023.9180011.

[66] M. B, M. B. Long-term durability of concrete structures. J Phys Conf Ser n.d.;1614:012006. https://doi.org/10.1088/1742-6596/1614/1/012006.

[67] Weiqi X, Vivian WY T, Khoa N L, Jian Li H, Jun W. Life cycle assessment of recycled aggregate concrete on its environmental impacts: A critical review. Constr Build Mater 2022;317:125950. https://doi.org/10.1016/j.conbuildmat.2021.125950.

[68] Abdinasir K, Madumita S, Otto D, Kim B, Agnes N. Combination of LCA and circularity index for assessment of environmental impact of recycled aggregate concrete. J Sustain Cem Mater 2023;12:1–12. https://doi.org/10.1080/21650373.2021.2004562.

[69] Eftekhar Afzali S, Ghasemi M, Rahimiratki A, Mehdizadeh B, Yousefieh N, Asgharnia M. Compaction and Compression Behavior of Waste Materials and Fiber-Reinforced Cement-Treated Sand. J Struct Des Constr Pract 2025;30. https://doi.org/10.1061/JSDCCC.SCENG-1643.

[70] G. H, S. A. M, V. M. J, J. L. P, A. F, A. H, et al. Environmental impacts and decarbonization strategies in the cement and concrete industries. Nat Rev Earth Environ n.d.;1:559–73. https://doi.org/10.1038/s43017-020-0093-3.

[71] Daniel C R, Pedro C R A A, Tongbo S, Vanderley M J. Influence of cement strength class on environmental impact of concrete. Resour Conserv Recycl 2020;163:105075. https://doi.org/10.1016/j.resconrec.2020.105075.

[72] Natt M. Cost-benefit analysis of the production of ready-mixed high-performance concrete made with recycled concrete aggregate: A case study in Thailand. Heliyon 2020;6:e04135. https://doi.org/10.1016/j.heliyon.2020.e04135.

[73] Noura A, Jayasree C. Cost-Benefit Analysis of Vibrated Cement Concrete and Self-Compacting Concrete Containing Recycled Aggregates and Natural Pozzolana. J Eng Res n.d.;11. https://doi.org/10.36909/jer.15999.

[74] Guiwen L, Jianmin H, Neng W, Wenjie D, Xuanyi X. Material Alternatives for Concrete Structures on Remote Islands: Based on Life-Cycle-Cost Analysis. Adv Civ Eng n.d.;2022:7329408. https://doi.org/10.1155/2022/7329408.